IEEE Photonics Journal
An IEEE Photonics Society Publication

Open Access

Push–Pull Optical Nonreciprocal Transmission in Cascaded Silicon Microring Resonators

Volume 5, Number 1, February 2013

Mu Xu
Jiayang Wu
Tao Wang
Xiaofeng Hu
Xinhong Jiang
Yikai Su, Senior Member, IEEE

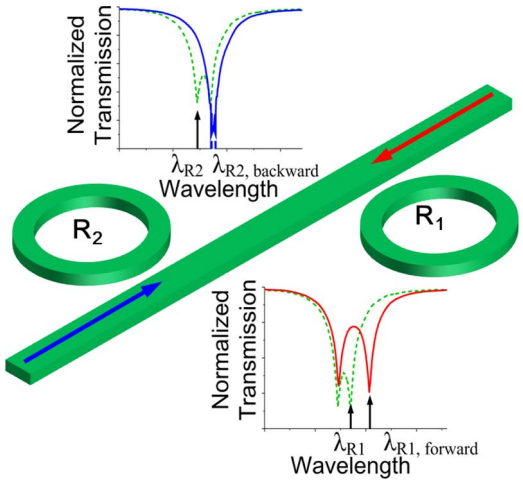

DOI: 10.1109/JPHOT.2013.2238665
1943-0655/$31.00 ©2013 IEEE

IEEE photonics SOCIETY

IEEE

Push–Pull Optical Nonreciprocal Transmission in Cascaded Silicon Microring Resonators

Mu Xu, Jiayang Wu, Tao Wang, Xiaofeng Hu, Xinhong Jiang, and Yikai Su, *Senior Member, IEEE*

State Key Laboratory of Advanced Optical Communication Systems and Networks, Department of Electronic Engineering, Shanghai Jiao Tong University, Shanghai 200240, China

DOI: 10.1109/JPHOT.2013.2238665
1943-0655/$31.00 ©2013 IEEE

Manuscript received December 5, 2012; revised January 3, 2013; accepted January 5, 2013. Date of publication January 9, 2013; date of current version February 4, 2013. This work was supported in part by the National Science Foundation of China under Grant 61077052 /61125504/61235007, by MoE Grant 20110073110012, and by the Science and Technology Commission of Shanghai Municipality under Grant 11530700400. Corresponding author: Y. Su (e-mail: yikaisu@sjtu.edu.cn).

Abstract: We experimentally demonstrate a push–pull optical nonreciprocal transmission (ONT) mechanism induced by thermo-optic effect in cascaded silicon microring resonators (MRRs). A nonreciprocal extinction ratio of up to 27 dB and an operation bandwidth larger than 0.15 nm are achieved in the proposed ONT system. The device can operate with a resonance mismatch between the two cascaded MRRs from 0.14 nm to 0.55 nm. The proposed ONT device could potentially find applications in optical diodes and bidirectional control of light in future on-chip all-optical information processing systems.

Index Terms: Silicon nanophotonics, optical nonreciprocal transmission (ONT), waveguide devices.

1. Introduction

Photonic devices with optical nonreciprocal transmission (ONT) property are useful to achieve certain functionalities in optical communication systems, such as optical diodes and circulators. However, breaking the time-reversal symmetry and integrating such devices onto micro photonic chips are challenging in both material integration and structure design. Several ONT devices relying on magneto-optic (MO) effect have been demonstrated [1]–[3], but the MO materials are difficult to be integrated on a complementary metal–oxide–semiconductor (CMOS) compatible photonic platform [4]. Devices based on indirect interband photonic transitions are also investigated [4], [5], but they rely on carrier injection or depletion effects bringing additional complexity in electrode layout and fabrication process. Fan *et al.* have demonstrated a one-way all-silicon passive optical diode based on optical nonlinear effect in cascaded silicon microring resonators (MRRs) [6]. However, in [6], the ONT response bandwidth is nearly equal to that of a microring notch filter, and the device needs two MRRs with identical resonance wavelengths. It is relatively sensitive to resonance mismatch induced by fabrication imperfections and thus requires more precise thermal tuning.

In this paper, we propose a compact ONT system based on cascaded MRRs on a silicon-on-insulator (SOI) platform. Unlike the devices with two resonance-matched resonators [6], [7], our device operates under resonance mismatch condition with a large tolerance from 0.1 nm to 0.5 nm. With thermo-optic (TO) effect, the mismatched cascaded MRRs can achieve push–pull resonance shifts for different input-signal directions, leading to a flat 0.15-nm operation bandwidth with 10-dB

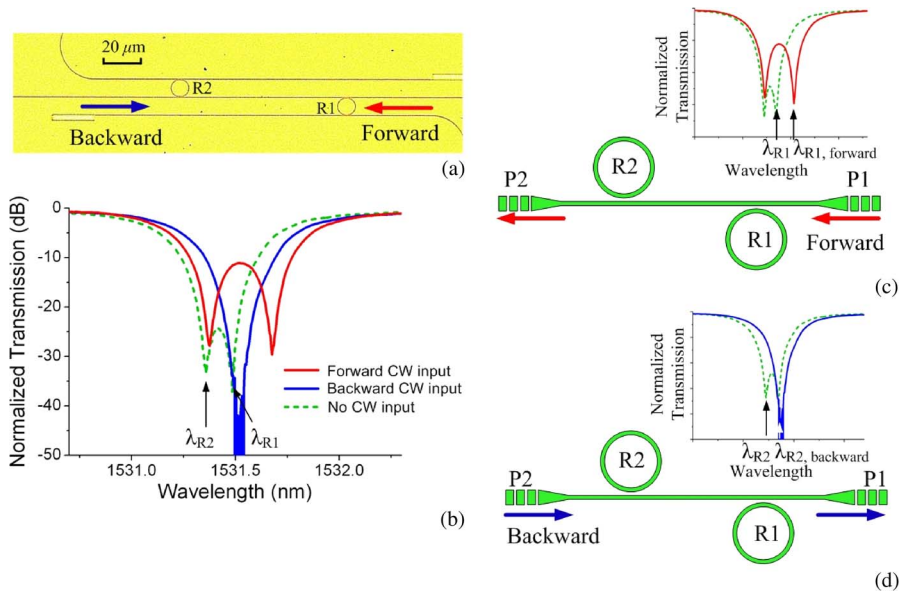

Fig. 1. Structure and operation principle of the cascaded MRRs based push–pull ONT system. (a) Micrograph of the ONT device. Forward and backward directions are marked by red and blue arrows, respectively. (b) Transmission spectra with no input, forward propagated, and backward propagated CW lights, respectively. λ_{R1} and λ_{R2} refer to the initial resonance wavelengths of MRR R_1 and R_2, respectively. (c) TO-effect-induced transmission change with forward input CW light redshifting λ_{R1} to $\lambda_{R1,forward}$. (d) TO-effect-induced transmission change with backward input CW light redshifting λ_{R2} to $\lambda_{R2,backward}$. All the transmission spectra are obtained from experimental results. The CW input light is fixed at a different resonance of 1539.26 nm. The power is 18.0 dBm at the end of the input fiber.

extinction ratio. The bandwidth is almost three times larger than that demonstrated in [6]. In the following section, experimental results are demonstrated, and a comparison between the ONT systems under push–pull and single-MRR operations is provided by simulations. The proposed ONT device could find applications such as optical diodes, optical transistors [8], and bidirectional all-optical control in future information processing photonic chips.

2. Device Structure and Operation Principles

The proposed ONT system consists of a pair of MRRs side-coupled to a straight waveguide as shown in Fig. 1(a). Theoretically, the resonance wavelengths of the two silicon MRRs with the same dimensions and coupling coefficients should be identical. However, a slight detuning is introduced between the resonances of the two cascaded MRRs as shown by the green dashed transmission curve in Fig. 1(b). The detuning between the two resonances is $\Delta\lambda = (\lambda_{R1} - \lambda_{R2})$, where λ_{R1} and λ_{R2} are the resonance wavelengths of MRR R_1 and R_2 with $\lambda_{R1} \geq \lambda_{R2}$, respectively.

With a continuous-wave (CW) light input, the TO effect dominates the free-carrier (FC) nonlinear effect within the MRR [9] thus leading to a red shift of the resonance wavelength. The resonance shift $\delta\lambda$ owing to the counteracting effects between TO and FC processes can be expressed as follows [10]:

$$\delta\lambda = \frac{\lambda_0}{n_g}(\delta n_{TO} + \delta n_{FC}) \approx \frac{\lambda_0}{n_g}\delta n_{TO} \tag{1}$$

where λ_0 is the resonance wavelength, n_g is the group index, and δn_{TO} or δn_{FC} is the silicon refractive index changes induced by TO or FC effect, respectively. The index change induced by thermal effect can be written as [11]

$$\delta n_{TO} = \Gamma_{th} k_{th} R_{th} \gamma_{abs} U \tag{2}$$

where Γ_{th} is the effective confinement factor corresponding to the TO effect, $k_{th} = 1.86 \times 10^{-4}$ K^{-1} is silicon TO coefficient, $R_{th} = 50$ K/mW is the thermal resistance of the silicon ring resonator, γ_{abs} is defined as the total resonator absorption rate including linear absorption, free-carrier absorption, as well as two photo absorption, and U is the resonator internal stored energy. With a CW input optical power P_{in} at a wavelength of λ, U can be simplified as [12]

$$U = P_{co}/\gamma_{abs} = \left(1 - |T(\lambda)|^2\right) P_{in}/\gamma_{abs} \tag{3}$$

where P_{in} is the input optical power, P_{co} is the power coupled from the bus waveguide, and $T(\lambda)$ is the transmission coefficient at the steady state. Equation (1)–(3) reveal that the thermo-induced resonance shift is proportional to the CW optical power injected into the silicon MRR.

With forward and backward directions labeled in Fig. 1, using (1)–(3), one can obtain the ratio between the resonance shifts of R_1 and R_2 for the forward propagation as

$$\frac{\delta\lambda_{R1,forward}}{\delta\lambda_{R2,forward}} \approx \frac{U_{R1,forward}}{U_{R2,forward}} = \frac{1}{\left|T_{R1,forward}(\lambda)\right|^2}\left[\frac{1 - \left|T_{R1,forward}(\lambda)\right|^2}{1 - \left|T_{R2,forward}(\lambda)\right|^2}\right] \tag{4}$$

where $U_{R1,forward}$, $U_{R2,forward}$, $T_{R1,forward}(\lambda)$, and $T_{R2,forward}(\lambda)$ represent the internal stored energies and the transmission coefficients of corresponding MRRs at steady state in forward direction, respectively. Since the input light passes R_1 with an attenuation factor $|T_{R1,forward}(\lambda)|^2$, less optical energy is injected and stored in the resonator R_2, resulting in a smaller resonance shift $\delta\lambda_{R2,forward}$ compared with $\delta\lambda_{R1,forward}$ as shown in Fig. 1(c). If the operation wavelength of CW input is set close to the resonance of R_1 with $|T_{R1,forward}(\lambda)|^2 \approx 0$, R_1 dominates the resonance shift process since the optical energy stored within R_2 is significantly attenuated. Similarly, with a CW backward input, one can obtain

$$\frac{\delta\lambda_{R1,backward}}{\delta\lambda_{R2,backward}} \approx \frac{U_{R1,backward}}{U_{R2,backward}} = \left|T_{R2,backward}(\lambda)\right|^2\left[\frac{1 - \left|T_{R1,backward}(\lambda)\right|^2}{1 - \left|T_{R2,backward}(\lambda)\right|^2}\right] \tag{5}$$

where $U_{R1,backward}$, $U_{R2,backward}$, $T_{R1,backward}(\lambda)$, and $T_{R2,backward}(\lambda)$ are the internal stored energies and transmission coefficients of the corresponding MRRs, respectively, with backward propagation. Light will be coupled into resonator R_2 first, which leads to a decreased optical energy passing R_2 and stored in R_1. Then, the resonance red shift of R_1 is consequently smaller than that of R_2 as shown in Fig. 1(d). When R_2 is on-resonance with $|T_{R2,backward}(\lambda)|^2 \approx 0$, $\delta\lambda_{R1,backward}$ becomes negligible compared with $\delta\lambda_{R2,backward}$. As a result, similar to a class-B push–pull power amplifier with only one of the two transistors conducting at a time [13], a push–pull ONT device is achieved with two cascaded MRRs, where one resonator dominates the resonance shift in the forward propagation direction and the other one dominates such process in the backward propagation direction. A comparison between transmission spectra for forward and backward propagation directions is shown in Fig. 1(b). The ONT effect is obtained in a wavelength range where forward transmission exceeds backward transmission.

3. Experimental Results and Discussions

The proposed device is fabricated on an 8-inch SOI wafer with a 220-nm-thick top silicon layer and a 2-μm-thick buried dioxide layer. A 248-nm deep ultraviolet photolithography is used to define the pattern followed by an inductively coupled plasma etching process to etch the top silicon layer. The radii of both silicon MRRs are $R \approx 5$ μm. The cross-section of the silicon waveguides is 450×220 nm^2, and the gap width in the coupling regions is 180 nm. Grating couplers are used at both ends of the bus waveguide to couple the transverse-electric (TE) polarized light between single-mode fibers (SMFs) and the on-chip ONT device. A 1.5-μm-thick silica layer is deposited to cover the whole device as upper cladding.

The experimental setup shown in Fig. 2 is exploited to measure the ONT performance of the fabricated device in the C band. A CW light emitted from a tunable laser is amplified by a high-power

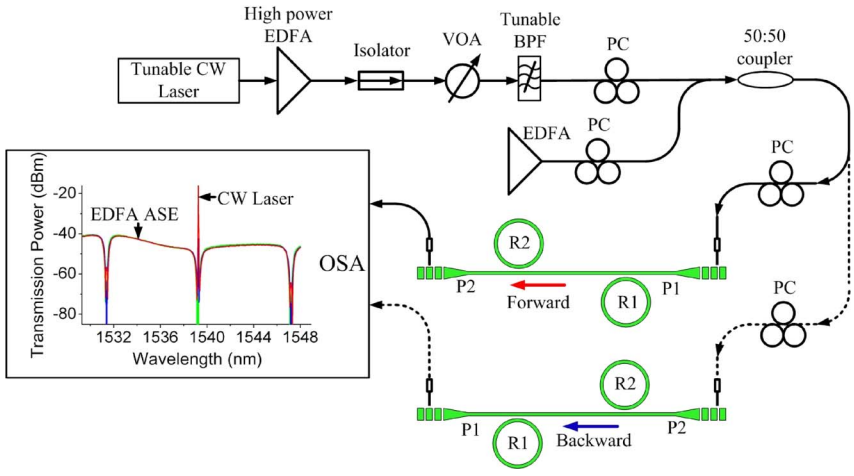

Fig. 2. Experimental setup of cascaded MRRs based ONT system. Forward and backward directions are marked by red and blue arrows, respectively. Inset shows the spectra composed of ASE and CW light displayed by OSA. EDFA: erbium-doped fiber amplifier; VOA: variable optical attenuator; BPF: bandpass filter; PC: polarization controller.

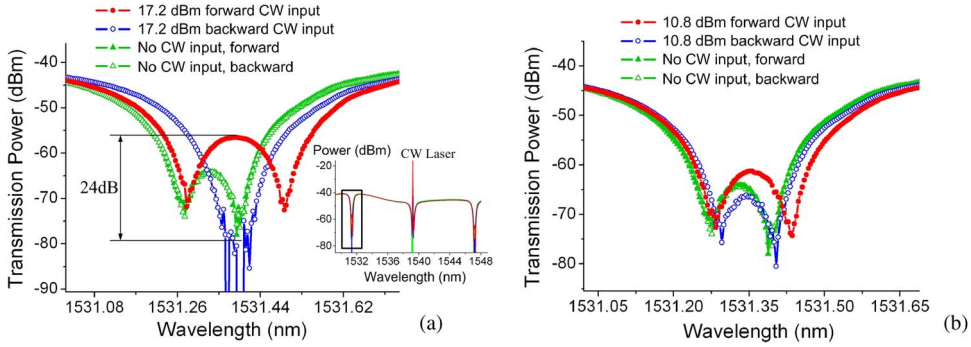

Fig. 3. Transmission spectra demonstrating the ONT effect with forward input (red solid circles), backward input (blue open circles), and no CW light input (green solid and open triangles). The power of the input CW light is set to (a) 17.2 dBm (∼8.2 dBm coupled into the device in consideration of 9 dB fiber-to-chip loss) and (b) 10.8 dBm (∼1.8 dBm coupled into the device). Inset in (a) shows the location of the chosen resonances marked by a black box in the displayed spectra.

erbium-doped fiber amplifier (EDFA) followed by a variable optical attenuator (VOA) to adjust the optical power. The high-power EDFA is used to compensate 9-dB fiber-to-chip loss induced by the vertical coupling system. Another EDFA provides a low-power broadband amplified spontaneous emission (ASE) to characterize the transmission spectra. The CW light and the ASE are combined through a 3-dB coupler and fed to the ONT device by the vertical coupling system. The wavelength of the CW light is carefully tuned near the resonances of the cascaded MRRs in order to observe ONT phenomenon. The output spectral responses are recorded and characterized by an optical spectrum analyzer (OSA) at a resolution of 0.02 nm.

Fig. 3 shows the measured forward and backward spectral responses demonstrating the resonance changes adjacent to the CW light input. Transmission spectra without CW light input are also depicted. As shown in Fig. 3(a), the initial resonance detuning between R_1 and R_2 is $\Delta\lambda_0 \approx 0.14$ nm. A redshift of resonance λ_{R1} from 1531.40 nm to 1531.52 nm is obtained when the forward CW input power is set to 17.2 dBm at the end of the input fiber with an operation wavelength of 1539.26 nm. An optical power of $\sim$ 8.2 dBm is injected into the device in consideration of 9-dB fiber to chip loss. Consequently, an increased resonance detuning of 0.24 nm is obtained. On the

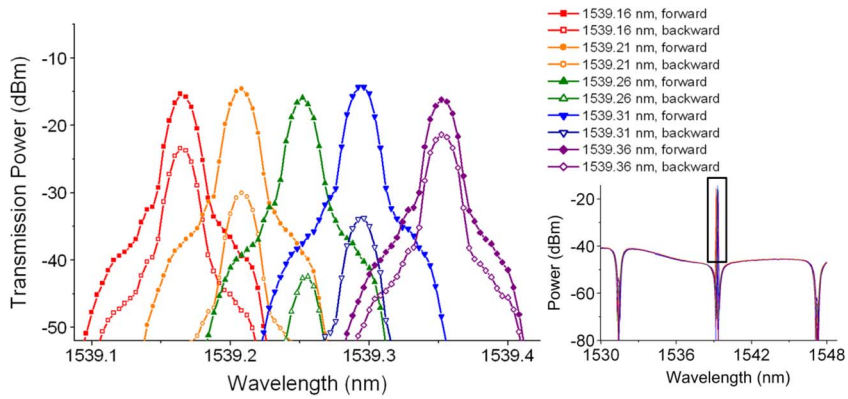

Fig. 4. Output power spectra of the forward and backward propagated CW light for various operation wavelengths with a fixed power of 17.2 dBm. A black open box is used to locate the CW light output at the measured spectra shown in the inset.

other hand, a 17.2-dBm backward CW light redshifts the resonance λ_{R2} from 1531.26 nm to $\sim$1531.39 nm and reduces the resonance detuning to less than 0.09 nm. The random fluctuations at the bottom of the resonance in Fig. 3(a) are possibly attributed to beating noise, environmental perturbations, thermal noise, and fluctuations in the pump power. We define nonreciprocal extinction ratio (NER) as a ratio between forward transmission $T_{\text{forward}}(\lambda)$ and backward transmission $T_{\text{backward}}(\lambda)$ with the same input CW light wavelength and power. A large NER of 24 dB is obtained by the push–pull nonreciprocal resonance shifts in Fig. 3(a). As shown in Fig. 3(b), when the injected optical power becomes lower, e.g., 1.8 dBm, NER decreases due to a smaller resonance shift induced by a relatively weaker TO effect.

The selected forward and backward output spectra of the CW light propagating through the proposed ONT system with a fixed power of 17.2 dBm are depicted in Fig. 4. An NER larger than 15 dB is achieved with CW light operation wavelength tuned from 1539.21 nm to 1539.31 nm, and a maximum value of $\sim$27 dB is achieved at 1539.26 nm. Since the proposed ONT system is based on silicon MRRs, the operational wavelength range is limited by their resonant bandwidths. As shown by the red and purple curves in Fig. 4, the NER of the ONT device is degraded when the operation wavelength is tuned away from 1539.26 nm where the strongest ONT effect takes place. Apart from the 18-dB coupling loss, the CW optical power is attenuated by 0.4-dB waveguide transmission loss (1-mm-long waveguide with an attenuation coefficient of 4 dB/cm). In addition, the loss induced by resonance notch is more than 12 dB, as shown in the inset in Fig. 4.

Fig. 5(a) presents the NER of the fabricated ONT device at different CW light input power with the wavelength fixed at 1539.26 nm. The initial resonance detuning between R_1 and R_2 is $\sim$ 0.14 nm. It can be seen that, due to the TO nonlinear effect, the overall NER spectrum redshifts with an improved extinction ratio as input power increases. When the input power is lower than 6.8 dBm, the TO-effect-induced resonance shift would become weaker, and the obtained NER is reduced to $\sim$5 dB. However, when the CW input power becomes higher, e.g., $>$ 15.5 dBm, the resonance wavelengths of R_1 and R_2 become closer to each other in the backward propagation direction, thus leading to an increased maximum NER, as well as a decreased ONT response bandwidth. The quality factor of the silicon MRRs, i.e., $Q = \lambda_0/\Delta\lambda$ [14], is estimated to be $\sim$3000, where λ_0 and $\Delta\lambda$ are the central wavelength and the 3-dB bandwidth of the resonance, respectively. Since the internal field enhancement factor in the cavity is proportional to Q [12], the power consumption of the ONT system could be reduced by sacrificing the operation bandwidth if the quality factors of the cascaded rings are increased, which can be realized by optimizing the micro fabrication parameters to reduce the surface roughness [15] or introducing nonetching processes to avoid intrinsic surface corrugation induced by etching [16].

The flat top of the NER spectrum curve is a result of the push–pull nonreciprocal resonance shifts. Fig. 5(b) provides the NER spectrum with the CW input power of 15.5 dBm and the

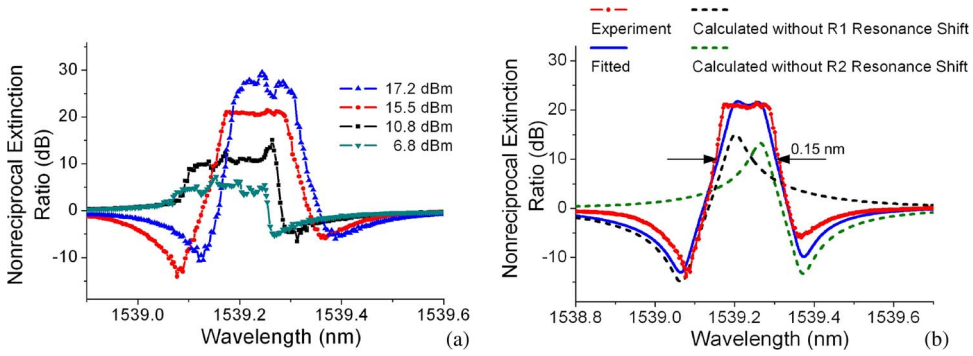

Fig. 5. (a) NER for various CW light input power with operation wavelength fixed at 1539.26 nm. (b) Measured (red dotted) and fitted NER (blue continuous) curves with an input optical power of 15.5 dBm at 1539.26 nm. The calculated NER curves ignoring the nonreciprocal resonance shifts of R_1 (black dashed) and R_2 (green dashed) are also depicted to compare with the NER induced by push–pull operation.

theoretically fitted curve. An operational bandwidth of 0.15 nm with NER larger than 10 dB is achieved. The calculation of the fitted curve is carried out by two steps: firstly, the TO-effect-induced resonance shifts are obtained from experiment results and based on the coupled mode theory [17], the forward and backward transmission functions of one MRR are obtained based on the following equations:

$$|T_R(\lambda)|^2 = \frac{4K^2(\lambda) + (1/Q_i - 1/Q_e)^2}{4K^2(\lambda) + (1/Q_i + 1/Q_e)^2} = \frac{4K^2(\lambda) + (1/Q_i - 1/Q_e)^2}{4K^2(\lambda) + (1/Q)^2} \tag{6}$$

where $K(\lambda) = (\lambda_0 + \delta\lambda - \lambda)/\lambda$ and Q_i or Q_e is the cavity quality factor related to the intrinsic loss or waveguide coupling loss, respectively. Then, the transmission spectrum of the cascaded MRRs is derived as $|T(\lambda)|^2 = |T_{R1}(\lambda)|^2 |T_{R2}(\lambda)|^2$. Secondly, the NER curve is achieved by calculating the ratio between the forward and backward transmission spectra. The initial resonance wavelengths of R_1 and R_2 are $\lambda_{0,R1} = 1539.24$ nm and $\lambda_{0,R2} = 1539.07$ nm, respectively. The corresponding resonance shifts are $\delta\lambda_{R1,forward} = 0.12$ nm, $\delta\lambda_{R2,forward} = 0.01$ nm, $\delta\lambda_{R1,backward} = 0.02$ nm, and $\delta\lambda_{R2,backward} = 0.12$ nm. The quality factors for resonator R_1 and R_2 are $Q_{i,R1} = 5900$, $Q_{i,R2} = 6000$, $Q_{e,R1} = 6800$, and $Q_{e,R2} = 6900$. As shown in Fig. 5(b), the fitted curve is approximately in agreement with the experimental result. To compare with an ONT system under single-MRR operation, we calculate the NER curve that ignores R_1 or R_2 resonance shift in the ONT process as depicted in Fig. 5(b) with other simulation parameters unchanged. Decreased maximum extinction ratios and reduced operation bandwidths are observed, indicating that the push–pull ONT mechanism could be an effective method to improve the response bandwidth and NER of the silicon MRR-based ONT device.

The device operation is tolerant to fabrication-induced resonance mismatch within a range from 0.14 nm to 0.55 nm. As shown in Fig. 6, with the operation wavelength of the CW light fixed at 1539.24 nm, nonreciprocal transmissions are also achieved for the proposed ONT devices with resonance detunings of 0.32 nm and 0.55 nm, respectively. Given such an operation window from 0.14 nm to 0.55 nm, one could use thermal heating pads to tune the resonances of the cascaded MRRs and ensure that the mismatch falls in this range. Meanwhile, the working wavelength, operation bandwidth, and NER of the proposed ONT system could also be adjusted by introducing such thermal tuning mechanism.

4. Conclusion

We have demonstrated a TO-effect-induced push–pull ONT mechanism in cascaded silicon MRRs. A mismatch (0.1 nm–0.5 nm) between the resonances of two MRRs is introduced for the device. With such a resonance mismatch, nonreciprocal resonance shifts have been achieved in both

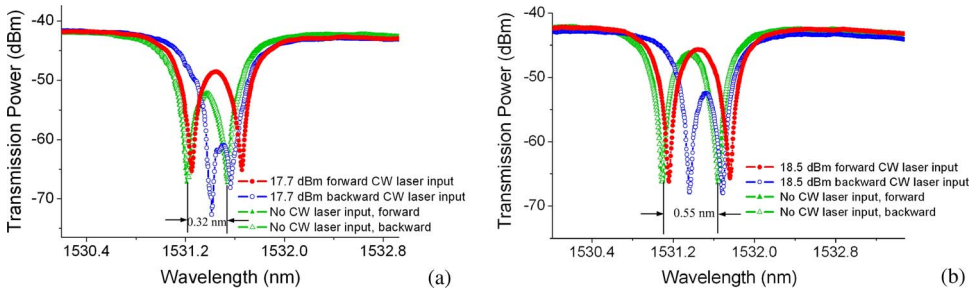

Fig. 6. Transmission spectra with forward CW light input (red solid circles), backward input (blue open circles), and no input (green solid and open triangles) for the proposed ONT systems with resonance detunings between R_1 and R_2 of (a) 0.32 nm and (b) 0.55 nm, respectively. The operation wavelength of the CW light is fixed at 1539.24 nm.

forward and backward propagation directions. By carefully tuning the wavelength and power of the CW light input, a maximum NER up to 27 dB has been obtained, as well as a relatively broad 10-dB operation bandwidth of 0.15 nm. The proposed device does not require external magnetic fields and electro-optical modulation. With a compact footprint and a simple architecture, the proposed ONT system could be a useful component in applications requiring nonreciprocal characteristics such as all optical diodes, optical transistors, and bidirectional control of light in future all optical signal processing chips.

References

[1] L. Bi, J. Hu, P. Jiang, D. H. Kim, G. F. Dionne, L. C. Kimerling, and C. A. Ross, "On-chip optical isolation in monolithically integrated non-reciprocal optical resonators," *Nat. Photon.*, vol. 5, no. 12, pp. 758–762, Dec. 2011.
[2] T. Mizumoto, R. Takei, and Y. Shoji, "Waveguide optical isolators for integrated optics," *IEEE J. Quantum Electron.*, vol. 48, no. 2, pp. 252–260, Feb. 2012.
[3] W. V. Parys, B. Moeyersoon, D. V. Thourhout, R. Baets, M. Vanwolleghem, B. Dagens, J. Decobert, O. L. Gouezigou, D. Make, R. Vanheertum, and L. Lagae, "Transverse magnetic mode nonreciprocal propagation in an amplifying AlGaInAs/InP optical waveguide isolator," *Appl. Phys. Lett.*, vol. 88, no. 7, pp. 071115-1–071115-3, Feb. 2006.
[4] Z. Yu and S. Fan, "Optical isolation based on nonreciprocal phase shift induced by interband photonic transitions," *Appl. Phys. Lett.*, vol. 94, no. 17, pp. 171116-1–171116-3, Apr. 2009.
[5] H. Lira, Z. Yu, S. Fan, and M. Lipson, "Electrically driven nonreciprocity induced by interband photonic transition on a silicon chip," *Phys. Rev. Lett.*, vol. 109, no. 3, pp. 033901-1–033901-5, Jul. 2012.
[6] L. Fan, J. Wang, L. T. Varghese, H. Shen, B. Niu, Y. Xuan, A. M. Weiner, and M. Qi, "An all-silicon passive optical diode," *Science*, vol. 335, no. 6067, pp. 447–450, Jan. 2012.
[7] T. Hu, H. Qiu, P. Yu, C. Qiu, W. Wang, X. Jiang, M. Yang, and J. Yang, "Wavelength-selective 4 $\times$ 4 nonblocking silicon optical router for networks-on-chip," *Opt. Lett.*, vol. 36, no. 23, pp. 4710–4712, Dec. 2011.
[8] L. T. Varghese, L. Fan, J. Wang, F. Gan, B. Niu, Y. Xuan, A. M. Weiner, and M. Qi, *A Silicon Optical Transistor*, Apr. 2012. [Online]. Available: http://arxiv.org/abs/1204.5515arXiv: physics-optics/1204.5515
[9] Q. Xu and M. Lipson, "Carrier-induced optical bistability in silicon ring resonators," *Opt. Lett.*, vol. 31, no. 3, pp. 341–343, Feb. 2006.
[10] L.-W. Luo, G. S. Wiederhecker, K. Preston, and M. Lipson, "Power insensitive silicon microring resonators," *Opt. Lett.*, vol. 37, no. 4, pp. 590–592, Feb. 2012.
[11] P. E. Barclay, K. Srinivasan, and O. Painter, "Nonlinear response of silicon photonic crystal microresonators excited via an integrated waveguide and fiber taper," *Opt. Exp.*, vol. 13, no. 3, pp. 801–820, Feb. 2005.
[12] H. Chen, X. Luo, and A. W. Poon, "Cavity-enhanced photocurrent generation by 1.55 μm wavelengths linear absorption in a p-i-n diode embedded silicon microring resonator," *Appl. Phys. Lett.*, vol. 95, no. 17, pp. 171111-1–171111-3, Oct. 2009.
[13] R. L. Boylestad and L. Nashelsky, *Electronic Devices and Circuit Theory,* 9th ed. Englewood Cliffs, NJ: Prentice-Hall, 2007, pp. 556–558.
[14] Q. Xu, V. R. Almeida, and M. Lipson, "Micrometer-scale all-optical wavelength converter on silicon," *Opt. Lett.*, vol. 30, no. 20, pp. 2733–2735, Oct. 2005.
[15] J. Niehusmann, A. Vörckel, P. H. Bolivar, T. Wahlbrink, W. Henschel, and H. Kurz, "Ultrahigh-quality-factor silicon-on-insulator microring resonator," *Opt. Lett.*, vol. 29, no. 24, pp. 2861–2863, Dec. 2004.
[16] A. Griffith, J. Cardenas, C. B. Poitras, and M. Lipson, "High quality factor and high confinement silicon resonators using etchless process," *Opt. Exp.*, vol. 20, no. 19, pp. 21 341–21 345, Sep. 2012.
[17] Q. Li, T. Wang, Y. Su, M. Yan, and M. Qiu, "Coupled mode theory analysis of mode-splitting in coupled cavity system," *Opt. Exp.*, vol. 18, no. 8, pp. 8367–8382, Apr. 2010.